Viscous Drag Reduction on Axisymmetric Bodies using Helical Riblets

A. R. Davari*
Department of Mechanical and Aerospace Engineering,
Science and Research Branch, Islamic Azad University, Tehran, Iran
E-mail: ardavari@srbiau.ac.ir
*Corresponding author

Received: 19 August 2014, Revised: 13 October 2014, Accepted: 14 October 2014

Abstract: A series of subsonic wind tunnel tests was conducted on an ogive-cylinder-flare configuration at zero angle of attack to study the effects of small helical protuberances on viscous drag reduction behavior. The experiments have been carried out on a smooth model and two wire-wrapped models with different spacing between the helical riblet rings, known as pitch length. In the present experiments, the pitch length to model diameter ratio for the wire-wrapped models were 0.5 and 1.0 and the velocity profiles at 19 streetwise locations as well as the pressure distribution on the model at the same positions have been measured and compared for the smooth model and the two wire-wrapped ones. The results show about 10% reduction in the local skin friction drag for the wire-wrapped model in comparison with the smooth one. The investigations also showed that depending on the boundary layer thickness, optimum values could be found for the riblet diameter and its pitch length for which, the maximum reduction would be achieved in the local friction drag.

Keywords: Momentum Thickness, Near Wall Flow, Riblet-Momentum Integral, Viscous Sublayer

Reference: Davar, A. R., "Viscous Drag Reduction on Axisymmetric Bodies Using Helical Riblets", Int J of Advanced Design and Manufacturing Technology, Vol. 7/ No. 4, 2014, pp. 111-118.

Biographical notes: A. R. Davari received his PhD in Aerospace Engineering from Sharif University of Technlogy in 2006. He is currently Assistant Professor at the Department of Mechanical and Aerospace Engineering, Science and Research Branch, Islamic Azad University of Tehran. Wing-body and body-ground interactions have been the topics of his recent papers published. His current research interest includes the new prediction and optimization methods and tools in aerodynamics such as neural networks, DOE/RSM and evolutionary algorithms, Experimental and Applied Aerodynamics, Data Prediction Methods, and applied flight mechanics.

1 INTRODUCTION

Energy conservation and improvements in aerodynamic efficiency demand the development of various methods of turbulent drag reduction on different types of vehicles. Especially in the recent years the turbulent drag reduction has been a main issue of concern [1-3]. Among the various passive drag reduction concepts which have been tested experimentally to date, the concept of using longitudinal riblet surfaces aligned in the streamwise direction seems to be promising and is also relatively simple to implement.

The concept of the viscous drag reduction technique using riblet surface has been examined experimentally by many investigators [4]. Among them, the micro-grooved riblet surface is believed to be one of the most promising methods for practical applications. Walsh [5] was the first to study skin-friction drag of the riblet wall systematically. He found that the triangular or scalloped riblet of which spacings are less than 25 viscous wall units can reduce the friction drag by up to 8%. Since then, many studies of the riblet surface were performed under various flow conditions and knowledge of the drag reduction characteristics has been extended.

Hot-wire and Laser-Doppler velocimetry measurements [6], [7] showed that the turbulent intensities and the Reynolds shear stress were reduced near the riblet surface. However, these techniques could not fully explore the turbulent statistics close to the riblet surface that had small spacing and height. Thus, the behavior of the statistics in the vicinity of the ribs remains unknown, and the mechanism of drag reduction is still an open question. In the recent years, the drag reduction problem in Iran has been a main issue of concern [8-10].

For the first time in 1976 it has been discovered that the small flow-aligned fences improve the turbulent structure of the boundary layer near the solid wall and consequently decrease the skin friction. The existing knowledge at that time showed that the near wall region in a turbulent boundary layer encompasses low speed regions. These regions of retarded flow develop and extend in streamwise direction and eventually lift up from the surface. The Reynolds stress in a turbulent boundary layer was known to be a result of eruption of these low speed regions above the surface. The small rectangular fences which restrict the near-wall flow are known as riblets. Poddar and Van Alta placed two riblet rings on an axisymmetric body and studied the associated boundary layer behaviour [11]. The spacing between these two riblets was five times the local boundary layer thickness. They have reported a considerable reduction in skin friction. They have also shown that such rings on the body can decrease the level of disturbances near the wall.

In a turbulent flow there is still little knowledge about the flow structure due to the complexities existing in the flow. Figure 1 shows some of the phenomena observed in a turbulent boundary layer. In the near-wall region, the fluid motion is still laminar and there is a steep velocity gradient near the wall. Far from the wall, the turbulent flow dominates. Investigations show that the near wall laminar region is not really laminar. As shown in Fig. 1, bulks of low-speed fluid near the surface lift up from the wall and enter the fully turbulent region and smash into small pieces. The mechanism for this motion is still unknown. However this phenomenon should be a consequence of the instability in the laminar region due to the microscopic surface roughness. Once a bulk of fluid moved up from the near wall region, its position will immediately be occupied by another high energy bulk from the upper region.

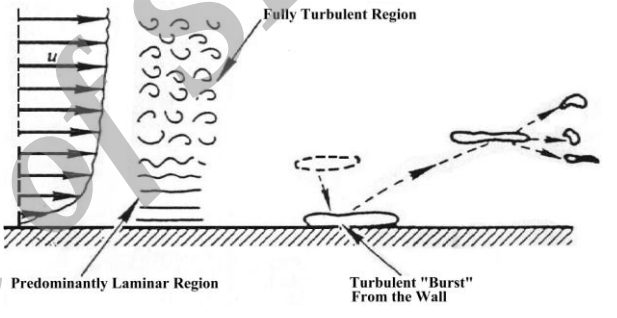

Fig. 1 The low-speed streaks motion near the wall [1]

Thus, the turbulence is a consequence of motion and breakdown of the bulks of fluid from the near wall to the outer region. This motion repeats in a certain period. Kline showed that the viscous sub layer has a streaky structure with local low speed streamwise regions [12]. Figure 2 shows a schematic view of the near wall flow. The thickness of these low speed streaks are about 30 to 40 wall units expressed as y^+. Thus the riblets height should be of the same order to inhibit the growth of these streaks.

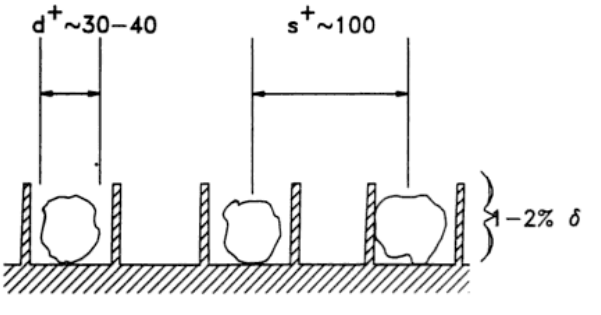

Fig. 2 The low speed streaks motion confined by the riblets

The size of the riblets is usually 1 to 2 percent of the local boundary layer thickness. The near-wall region plays an important role in generating the turbulence energy. The measurements show that more than 50% of the turbulence energy is generated in less than 2.5% of the boundary layer thickness.

On this basis, Liu showed that the longitudinally ribbed surface improves the near wall structure and decreases the skin friction [13]. He measured the burst frequencies of the low speed streaks pulling up in to the fully turbulent region. They found that when the spacing between two adjacent riblets, s^+, is less than 100 wall units, a considerable change in the burst frequency can be observed. This suggests that $s^+<100$ is a suitable range to limit the motion of the low speed streaks.

In the recent years, in spite of devising more advanced drag reduction techniques [14-16], riblets are still favorite tools to reduce the skin friction on the vehicles. Up to now, valuable information has been obtained about the riblets [17-19]. However, there is still a long way to understand the drag reduction mechanism of the riblets and the laws governing it. Among the various studies on riblets, to the author's knowledge, less were devoted to the mean flow variations and the boundary layer thickness parameters as well as the effects of riblet spacing on its effectiveness. In this paper, the impact of the riblet pitch-to-diameter ratio was studied on the friction drag of an axisymmetric body at zero angle of attack in a subsonic wind tunnel. The previous studies were mainly concentrated on the turbulence intensity which has been shown to decrease when using riblets. However, in the present studies, the mean values of velocity and pressure in the boundary layer were measured and compared for the smooth model and two wire-wrapped models with different riblet spacings. The amount of drag reduction in the wire-wrapped models comparing to the smooth configuration was then studied.

2 MODEL AND EXPERIMENTAL APPARATUS

The experiments were conducted in a closed circuit low speed wind tunnel whose cross sectional area was 60 cm × 60 cm with a test section length of 200 cm. The free stream velocity in this tunnel could be varied from 5 to 40 m/sec. Three layers of honey comb were provided for this tunnel to reduce the free stream fluctuations and deliver a uniform flow.

The model constructed for the present experiments was of an ogive-cylinder-boat tail combination with a length-to-diameter ratio of 13.18. Twenty pressure tabs were carefully drilled on the surface of the body. The tabs spacing was constantly 5.2 cm. To achieve a fully turbulent boundary layer over the model, a mild sand paper with a width of 10 cm was attached to the beginning of the cylindrical body. Figure 3(a) shows the schematic view of the model. Figures 3(b) and 3(c) show a schematic view of the wire-wrapped models. The experiments were performed at a constant velocity of 20 m/sec corresponding to a Reynolds number of 1.3×10^6 based on model length.

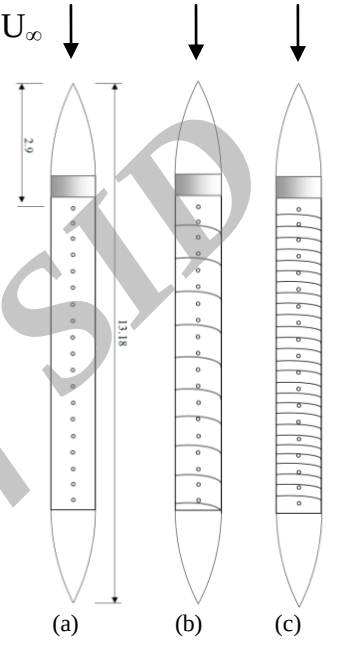

Fig. 3 The Schematic view of the models (dimensions are in caliber), (a) Smooth Model, (b) wrapped model with a pitch ratio of 1.0, (c) Wire-wrapped model with a pitch ratio of 0.5

In the present experiments, the surface pressure distribution along with the velocity profiles at 20 streamwise locations was measured. A steel L-shaped pitot tube with the internal and external diameters of 0.5 and 1 mm respectively, was used to read the velocity profiles. The pitot was mounted on a traversing system which allowed it to move both streamwise and transverse with a minimum increment of 1 mm. Regarding the area blocked by the model, since the experiments were all at zero incident angle, the maximum associated blockage ratio was measured to be 2.8%.

A steel wire of 0.5 mm in diameter has been wrapped helically around the model to modify the turbulent boundary layer structure and reduce the friction drag in the present studies. The distance between two adjacent wires divided by the model diameter is known as pitch to diameter ratio or simply pitch ratio. Two different pitch ratios of 0.5 and 1.0 were examined. If p denotes the spacing between two adjacent wires and D is the model diameter, to maintain a constant pitch to diameter ratio of p/D=0.5, it can easily be obtained

from geometry that the angle of the wires with respect to the horizon should be 80.96 and for p/D=1.0, this value should be 72.34 degrees.

3 RESULTS

Diagrams shown in Fig. 4 are the velocity profiles at various streamwise stations located at the front, middle and the rear parts of the model for the three cases; smooth model, wire-wrapped with p/D=0.5 and that with p/D=1.0. From this figure the effects of riblets and their pitch ratio on the boundary layer structure is evident at the rear region of the body while no meaningful change in the profiles shape can be observed at the front half. Since the laminar oncoming flow has been triggered by a mild sand paper at the beginning of the body, it is likely that a fully turbulent boundary layer has been established at about x/D=3.0 and the effectiveness of the riblets in re-laminarization process has been highlighted from that on.

This is clearly shown in Fig. 5, where the streamwise velocity distribution immediately after the wall has been shown for the smooth model and the wire-wrapped ones. The mean velocity values in the wire-wrapped profiles are less than those in smooth case and the velocity in the higher pitch ratio profile, i.e. p/D=1.0 is lower than that in p/D=0.5 case. In general, the lower the velocity near the wall, the lower will be the turbulence intensity within the boundary layer. On this basis, it can be inferred that the boundary layer behavior especially at the rear part of the wire-wrapped model is closer to a completely laminar profile than the smooth model case.

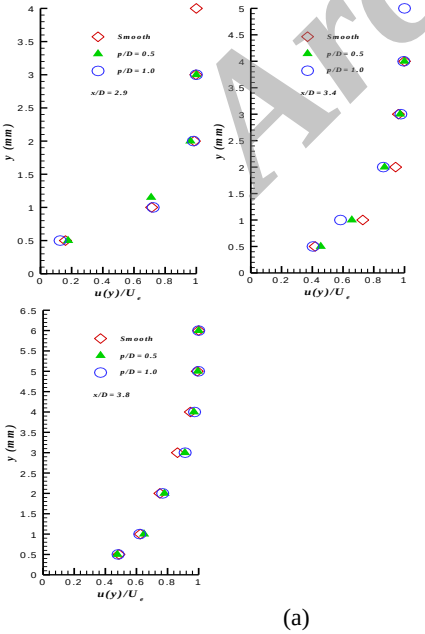

(a)

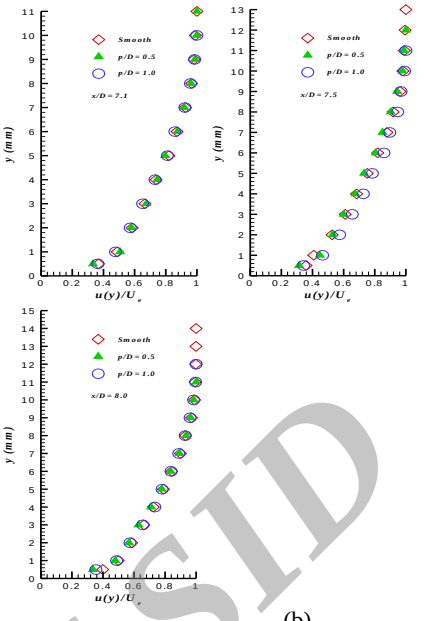

(b)

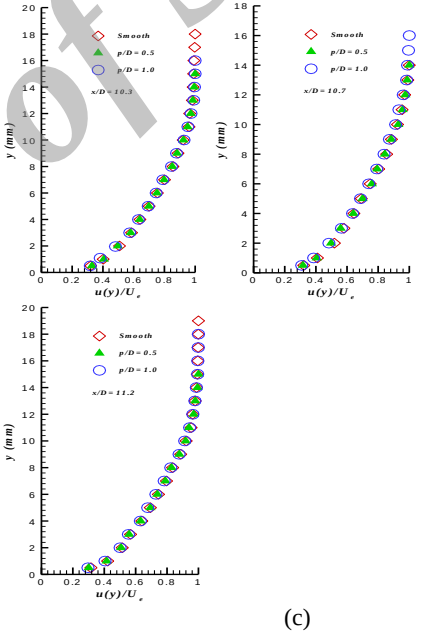

(c)

Fig. 4 The streamwise velocity profiles at different points along the body (a) The first three points, (b) The Three mid points, (c) The last three points

Moreover, the pitch to diameter ratio of 1.0 has shown to be more successful in re-laminarization process than p/D=0.5. Figure 6 shows the velocity profiles in terms of the non-dimensional wall functions u^+ and y^+ for the last four points on the model. For p/D=1.0 case, the riblets height in terms of y^+ at these points were 22.3, 20.45, 18.85 and 18.75 respectively, which have been specified on the profiles. Since y^+ is directly proportional to the wall shear stress, decreasing the values of y^+ from x/D=9.4 to x/D=10.7 is an indication

of shear stress reduction, as was expected. From this figure a reduction in u^+ for the wire-wrapped models are more pronounced, especially for p/D=1.0. This approves that the streamwise velocity variations in boundary layer for the wire-wrapped model with p/D=1.0 is closer in shape to a laminar profile comparing to the p/D=0.5 case.

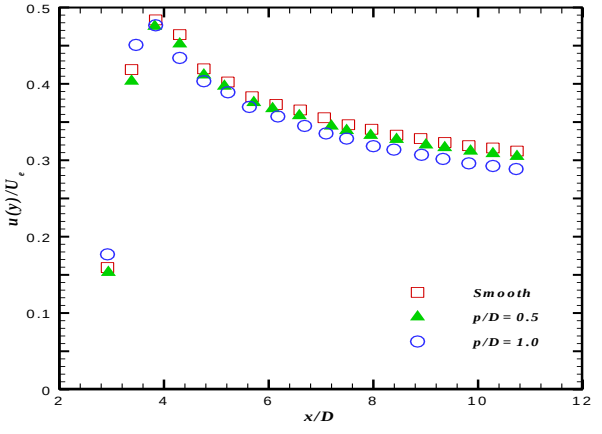

Fig. 5 Near-wall velocity distribution along the model

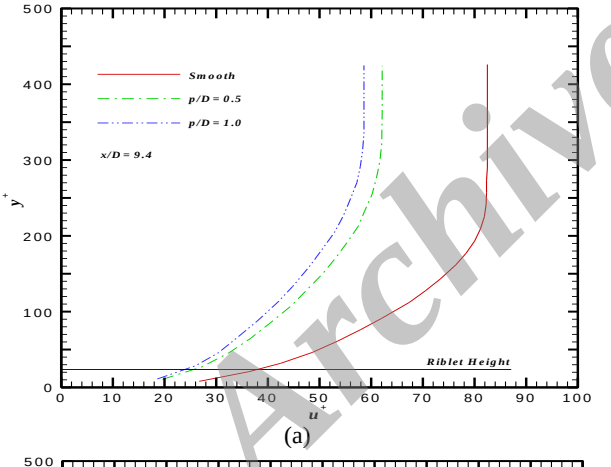

(a)

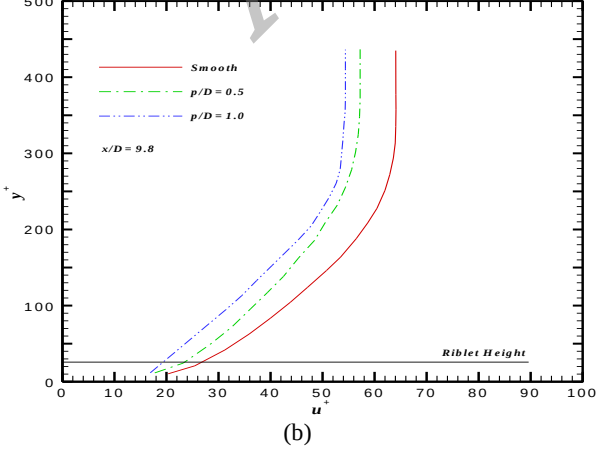

(b)

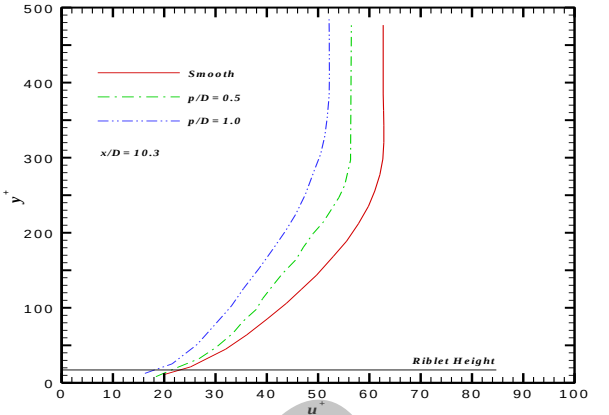

(c)

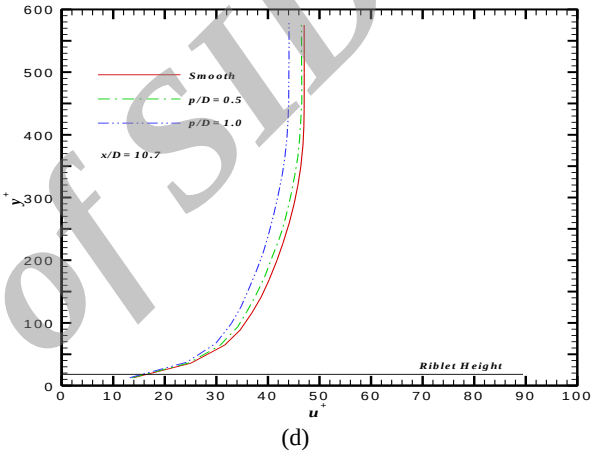

(d)

Fig. 6 Velocity profiles at the last four streamwise points on the model in terms of the non-dimensional wall variables, (a) x/D=9.4, (b) x/D=9.8, (c) x/D=10.3, (d) x/D=10.7

The longitudinal pressure distribution on the model is shown in Fig. 7. For the three cases examined here, the pressure coefficient decreases until about x/D=3.0 and then increases until about x/D=4.5. It is likely that a fully turbulent flow has not been completely established in this range.

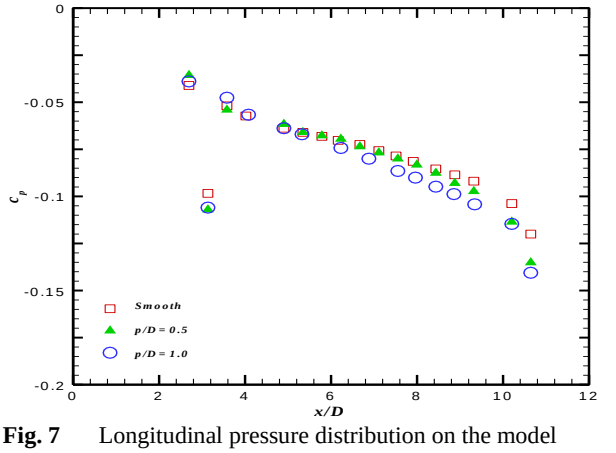

Fig. 7 Longitudinal pressure distribution on the model

For the values of x/D more than 4.5, the pressure coefficient exhibits a descending behavior for the three cases. However, this value for the wire-wrapped model with a pitch ratio of 1.0 is less than the two other cases. The drop in c_p for x/D>4.5 is associated with a decrease in Δp. The lower the pressure difference the higher would be the near wall velocity. As a consequence of reduction in the velocity gradient near the wall, the skin friction decreases.

Figures 8 and 9 show the streamwise distribution of the boundary layer displacement thickness and momentum thickness on model for the three cases examined in the present experiments. The boundary layer thickness for the smooth model at the first and the last measuring points were 4 and 19 mm. For this model, the values of boundary layer thickness and the momentum thickness were 1.3 mm and 0.2 mm at the first point and also 4.2 mm and 2.2 mm for the last point respectively.

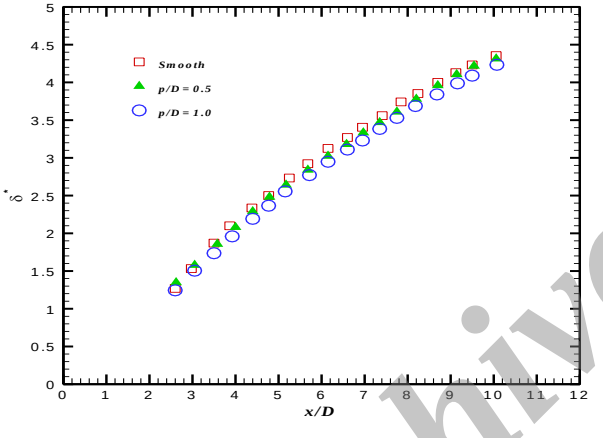

Fig. 8 The streamwise distribution of the boundary layer displacement thickness along the model

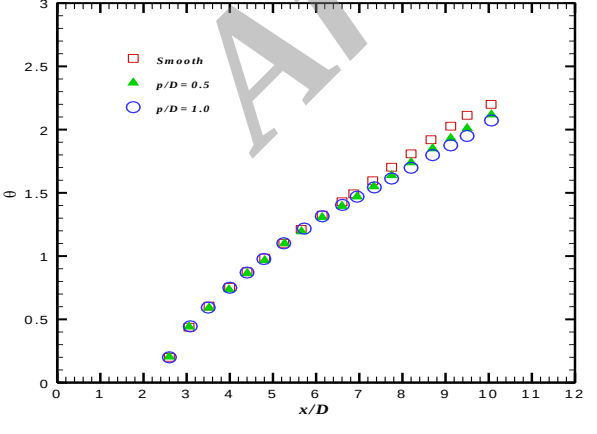

Fig. 9 The streamwise distribution of the boundary layer momentum thickness along the model

According to these figures, the values of the displacement thickness and the momentum thickness for the wire-wrapped models are lower than the corresponding values on the smooth configuration. This indicates that the energy dissipation due to boundary layer effects for the wire-wrapped cases is less than the smooth model. Both figures also approve that the wire-wrapped model with a pitch ratio of 1.0 has more successfully re-laminarized the profile than the p/D=0.5 case.

The slope of the momentum thickness with respect to x, i.e. $d\theta/dx$ at the last measuring point for instance was 0.00194 for the smooth model, 0.00179 for p/D=0.5 and 0.00169 for p/D=1.0. As an approximation, the flow on the surface of the model can be considered to be similar to a flat plate flow of infinite length. In this case, knowing $d\theta/dx$, the values of skin friction coefficients can be calculated from the momentum integral equation. These results are summarized in Table 1.

Table 1 The values of c_f for the last point

Case	c_f
Smooth	0.00388
p/D=0.5	0.00358
p/D=1.0	0.00338

From these data, the reduction in the skin friction coefficient is evident. At the last measuring point, the reductions in c_f for the wire-wrapped model with p/D=0.5 and that with p/D=1.0 were 8 and 13 percent respectively. An uncertainty analysis on velocity measurement data shows an average error of about 3 percent. On this basis, the minimum reduction in the friction drag coefficient for the two wire-wrapped configurations comparing to the smooth model can be estimated to be about 5 and 10 percents for the p/D=0.5 and the p/D=1.0 cases respectively.

In the present experiments, y^+=100 corresponds to y= 0.176 cm for the wire-wrapped models. This means that the spacing between two adjacent riblet rings in the present experiments for p/D=0.5 and p/D=1.0 in terms of wall unit corresponds to y^+=32.1 and 64.2 respectively. Furthermore, as stated earlier, in the near-wall region of a turbulent boundary layer, the low speed streaks mostly exist up to about y^+=40. On this basis, the ratio of the low speed streaks height to the riblets diameter in the present experiments is about 3.0. Thus, to control the low speed streaks in the present experiments, the diameter of the riblets could be increased by 300 percent and the riblets spacing could be decreased down to 0.2 times the model diameter.

5 CONCLUSION

An experimental study has been undertaken on an axisymmetric body at zero angle of attack to study the effects of small fences placed within the boundary layer, on drag reduction. The results show that the riblets could successfully reduce the skin friction drag and a pitch length to diameter ratio of 1.0 worked better and more effective than that of 0.5. According to the results, in a fully turbulent flow using these thin riblets whose diameter is of order 1 to 2 percent of the boundary layer thickness, the momentum thickness for wire-wrapped axisymmetric bodies start to decrease from x/D>7.0 and for p/D=1.0; the amount of this drop is more pronounced than p/D=0.5.

The skin friction drag calculated from the momentum thickness distribution shows about 10 percent reduction in skin friction for p/D=1.0 and about 5 percent for p/D=0.5 comparing to the smooth model. On this basis, adding small helical protuberances on the smooth surface of an axisymmetric body for high Reynolds number motions such as a torpedo under water or a projectile in the air, would be effective in friction drag reduction, provided that the vehicle stability considerations are taken into account.

6 NOMENCLATURE

x	Longitudinal coordinate measured from apex	c_p	Pressure coefficient= $\frac{p-p_\infty}{\frac{1}{2}\rho U^2}$
y	Lateral coordinate measured from the model surface	v^*	Wall-friction velocity= $\sqrt{\frac{\tau}{\rho}}$
U	Free stream velocity	u^+	Inner wall velocity= $\frac{u(y)}{v^*}$
U_e	Longitudinal velocity at the edge of the boundary layer	y^+	Inner wall lateral coordinate = $\frac{yv^*}{\upsilon}$
υ	Kinematic viscosity	θ	Boundary layer Momentum Thickness
$u(y)$	Longitudinal velocity distribution inside the boundary layer	δ^*	Boundary layer displacement Thickness
τ	Wall shear stress	p	Spacing between two adjacent riblet rings
c_f	Skin friction coefficient= $\frac{\tau}{\frac{1}{2}\rho U^2}$	D	Model diameter
d^+	The low speed streaks diameter in wall scale	s^+	Riblets spacing in wall scale

REFERENCES

[1] Hemmasian, M. M. Rad, M., "Drag-Reduction Characteristics in Air Flow over the Iced Surface at Re>104", International Journal of Advanced Design and Manufacturing Technology, Vol. 1, No. 2 , 2008.

[2] Daneshmand, S., "Investigation of Surface Roughness on Aerodynamic Characteristics of Missiles", International Journal of Advanced Design and Manufacturing Technology, Vol. 4, No. 1, 2010.

[3] Barzanooni, V., "Experimental Investigation of the Aerodynamic of a Car Model", International Journal of Advanced Design and Manufacturing Technology, Vol. 6, No. 1, 2013.

[4] Walsh, M. J., "Riblets", AIAA Progress in Aeronautics and Astronautics: Viscous Drag Reduction in Boundary Layers, Vol. 123, 1990, pp. 203-261.

[5] Walsh, M. J., "Turbulent Boundary Layer Drag Reduction Using Riblets", AIAA Journal, Jan. 1982, pp. 82-0169.

[6] Park, S. R., Wallace, J. M., "Flow Alteration and Drag Reduction by Riblets in a Turbulent Boundary Layer", AIAA Journal, Vol. 32, No. 1, 1994, pp. 31-38.

[7] Benhalilou, M., Anselmet, F., and Fulachier, L., "Experimental Investigation of a Turbulent Boundary Layer Manipulated by a Ribbed Surface", Proceedings of the 9th Symposium on Turbulent Shear Flows, Kyoto University, Japan, Aug. 1993, pp. P107.1-P107.4.

[8] Hemmasian, M. M., Rad, M., "Drag-Reduction Characteristics in Air Flow over the Iced Surface at Re>104", International Journal of Advanced Design and Manufacturing Technology, Vol. 1, No. 2, 2008.

[9] Daneshmand, S., "Investigation of Surface Roughness on Aerodynamic Characteristics of Missiles", International Journal of Advanced Design and Manufacturing Technology, Vol. 4, No 1., 2010.

[10] Barzanooni, V., "Experimental Investigation of the Aerodynamic of a Car Model", International Journal of Advanced Design and Manufacturing Technology, Vol. 6, No. 1, 2013.

[11] Van Atta, C. W., Poddar, K., "Scaling and Structure Functions in Turbulent Shear Flows", Non-Linear Variability in Geophysics, Schertzer, D., and Lovejoy, S., (ed.), Springer Science & Business Media, 1991.

[12] Kline, S. J., Strawn, R. C., and Bardina, J. G., "Correlation of the detachment of two-dimensional turbulent boundary layers", AIAA Journal, Vol. 21, No. 1, 1983, 1983, pp. 68-73.

[13] Liu, C. K., Kline, S. J., and Johnson, J. P., "An Experimental Study of Turbulent Boundary Layers on Rough Walls", Thermo-scientist Division, Mechanical Engineering Department, Report MD-8, Stanford University, 1963.

[14] Bai, H. L., Zhou, Y., Zhang, W. G., Xu, S. J., Wang, Y. and Antonia, R. A., "Active control of a turbulent boundary layer based on local surface perturbation," Journal of Fluid Mechanics, Vol. 750, July 2014, pp. 316-354.

[15] Kim, Y. W., Lee, J. M., Lee, I., Lee, S. H., and Ko, J. S., "Skin friction reduction in tubes with

hydrophobically structured surfaces", International Journal of Precision Engineering and Manufacturing, Vol. 14, No. 2, 2013, pp. 299-306.

[16] Ahmed, M. Y. M., Qin, N., "Drag Reduction Using Aero disks for Hypersonic Hemispherical Bodies", Journal of Spacecraft and Rockets, Vol. 47, No. 1, 2010, pp. 62-80.

[17] Ng, J. H., Jaiman, R. K., "Direct Numerical Simulation of Geometric Effects on Turbulent Flows over Riblets", AIAA paper, AIAA 2014-2649, 7th AIAA Flow Control Conference, Atlanta, GA, 2014.

[18] Mohammadi, A., Floryan, J., "Pressure losses in grooved channels", Journal of Fluid Mechanics, Vol. 725, 2013, pp. 23-54.

[19] Campitelli, G., Krastev, V. K. and Huebsch, W., "Effects of Moving Surface Riblets on a Transitional Flow affected by Adverse Pressure Gradient", AIAA 2014-2651, 2014.